Supramolecular Complexes of MHC Class I, MHC Class II, CD20, and Tetraspan Molecules (CD53, CD81, and CD82) at the Surface of a B Cell Line JY[1]

János Szöllősi,* Václav Hořejší,[2†] László Bene,* Pavla Angelisová,† and Sándor Damjanovich[3*]

The results of previous biochemical studies indicated that a fraction of MHC class II proteins is associated with four proteins of the tetraspan family, CD37, CD53, CD81, and CD82, and possibly with other membrane components, at the surface of JY B lymphoma cells. In the present communication we used a biophysical technique, namely the flow cytometric energy transfer method, to demonstrate the proximity of these molecules at the surface of the cells. Significant energy transfer (and, therefore, proximity within the 2–10 nm range) was observed between fluorescently labeled mAbs to DR, DQ, and the tetraspan molecules CD53, CD81, and CD82. Moreover, two other B cell surface molecules, CD20 and MHC class I, were found to be close to each other and to MHC class II and the tetraspan proteins, based on the observed high energy transfer efficiencies between the relevant fluorescently labeled mAbs. The character of simultaneous energy transfer from CD20, CD53, CD81, and CD82 to DR suggests that all these molecules are in a single complex with the DR molecules (or a complex of several DR molecules) rather than that each of them is separately associated with different DR molecules. Based on these data and previous biochemical results, a model is proposed predicting that the B cell membrane contains multicomponent supramolecular complexes consisting of at least two MHC class I and at least one DR, DQ, CD20, CD53, CD81, and CD82 molecules. Closer analysis of the energy transfer efficiencies makes it possible to suggest mutual orientations of the components within the complex. Participation of other molecules, not examined in this study (CD19 and CD37), in these supramolecular structures cannot be ruled out. These large assemblies of multiple B cell surface molecules may play a role in signaling through MHC molecules and in Ag presentation to T cells. *The Journal of Immunology,* **1996, 157: 2939–2946.**

In recent years several structurally similar leukocyte surface proteins have been identified, which now constitute the tetraspan (or transmembrane 4) superfamily. Its members are distinguished by a polypeptide chain of approximately 200 to 300 amino acid residues containing four conserved hydrophobic, presumably transmembrane, domains. Both the C- and N-terminals are located intracellularly; a major extracellular loop of the polypeptide chain between the third and the fourth transmembrane domain is usually *N*-glycosylated on one or more sites and contains a characteristic strongly conserved cysteine motif. Individual members of this family differ widely in their expression: CD9 is characteristic for platelets and pre-B cells, CD37 is most strongly expressed on B lymphocytes, CD53 is a pan-leukocyte Ag, CD63 is a ubiquitous component of lysosomal membranes and appears on the surface of activated and tumor cells, CD81 and CD82 are broadly expressed on various leukocytes and other cell types, and CO-029 is found on carcinomas (for a review, see Ref. 1).

To date, little is known about the biologic roles played by these proteins. Their structure might suggest that they are involved in membrane transport of some ions or molecules, but this idea has no experimental support. Cross-linking of most of these proteins by suitable mAbs elicits marked biologic effects in the cells carrying them, including cell aggregation, activation, growth inhibition, or proliferation, depending on the cells, mAbs, and assays used (reviewed in Ref. 1). CD82 has recently been shown to be identical with a suppressor of prostate tumor metastases, but the molecular basis of this activity is unclear (2). The level of CD9 expression is also related to the metastatic potential (3).

A striking feature of most tetraspan proteins is their association with other membrane proteins: CD9 is linked to β_1 integrins (4), CD63 may be a component of the IgE-receptor complex (5), CD53 was reported to be associated with CD2 in rat activated T cells and NK cells (6), and CD81 and CD82 are associated with CD4 and CD8 coreceptors (7). CD81 was found to be a component of a B cell surface receptor complex involving CD21 (complement receptor type 2), CD19 and Leu 13 (8–11), and MHC class II (12). A recent report from our laboratory indicated that four tetraspan molecules (CD37, CD53, CD81, and CD82) were components of a complex (or several similar, structurally somewhat heterogeneous complexes) involving MHC class II and probably also CD19 and CD21. These results were obtained on the basis of experiments involving solubilization of B cell line membranes in the presence of mild detergents and immunoisolation by means of mAbs to

*Department of Biophysics, Medical University School, Debrecen, Hungary; and †Institute of Molecular Genetics, Academy of Sciences of the Czech Republic, Prague, Czech Republic

Received for publication February 8, 1996. Accepted for publication July 22, 1996.

The costs of publication of this article were defrayed in part by the payment of page charges. This article must therefore be hereby marked *advertisement* in accordance with 18 U.S.C. Section 1734 solely to indicate this fact.

[1] This work was supported by OTKA Grants 6163, 6221, 17592, and F0220590 (to L.B., S.D., and J.S.) and the Hungarian Scientific Board of Health (ETT) Grant T-05-477/93. The work of P.A. and V.H. was supported in part by Grants GA CR 310/93/0207 and 310/96/0673, a collaborative grant from Austrian Ministry of Science and Research, and a collaborative grant from the PECO program of ECC.

[2] Supported in part by an International Research Scholar's award from the Howard Hughes Medical Institute.

[3] Address correspondence and reprint requests to Dr. Sándor Damjanovich, Department of Biophysics, University Medical School, Nagyerdei Krt. 98, P.O. Box 39, H-4012 Debrecen, Hungary.

0022-1767/96/$02.00

various components of these complexes (13). This approach, however, suffers from inherent limitations due to the possible effects of detergents that may cause changes in the composition of the complexes compared with the situation in situ in native membranes. Therefore, in the present study we examined whether the previous biochemical results correlate with the data obtained by flow cytometric energy transfer (FCET).[4] This latter is a biophysical method probing the proximity of molecules on the cell surface on a cell by cell basis, under conditions very close to the physiologic state of the cells (14–20).

Thus, in this study we tried to determine which molecules are potential components of the B cell surface complexes containing tetraspan molecules and what are the possible mutual orientations of components of these complexes. In addition to some of the molecules suspected on the basis of previous experiments to be members of these complexes (MHC class II, CD53, CD81, and CD82), we also looked at others that are expressed at relatively high density in the B cell line used (MHC class I, CD20, and CD71 (transferrin receptor)) to determine whether some of them may also be components of supramolecular membrane complexes.

Materials and Methods

Cells

The JY B-lymphoma cell line was originally described by Terhorst et al. (21) and was maintained in RPMI 1640 medium supplemented with 10% FCS and antibiotics. The cells were harvested in the logarithmic phase of growth.

Monoclonal antibodies

mAbs W6/32 (against MHC class I; IgG2a), L368 (against β_2m; IgG1), Leu10 (against DQ; IgG1), and L243 (against DR; IgG2a) were all kindly provided by Dr. Frances Brodsky (University of California, San Francisco, CA); mAb BBM.1 (against β_2m; IgG2b), the HB28 hybridoma cell line secreting BBM.1, was a kind gift from Dr. Michael Edidin (The Johns Hopkins University, Baltimore, MD); mAb anti-CD71 (against CD71/transferrin receptor; IgG1) was a gift from Dr. Jef Rausch (Dr. Willem's Institute, Limburgs University Center, Diepenbeek, Belgium); mAbs M38 (against CD81; IgG2a) and C33 (against CD82; IgG2a) were kindly provided by Dr. Oshamu Yoshie (Shingoi Institute, Osaka, Japan); mAbs MEM-97 (against CD20; IgG1), MEM-137 (against DRα; IgG1), MEM-53 (against CD53; IgG1), and MEM-112 (against CD54; IgG1) were prepared and characterized in the authors' laboratory (Prague, Czech Republic).

Fab preparation

The Fab fragments were prepared from mAbs using the method previously reported (22). The main steps of preparation were the following. Dialysis of IgG was performed in a phosphate buffer (containing 100 mM Na_2HPO_4, 150 mM NaCl, and 1 mM EDTA) at pH 8, then digestion of the dialyzed IgG was conducted with papain activated in the presence of L-cysteine at 37°C for 11 to 11.5 min. The digestion was terminated with iodoacetamide, then the mixture was fractionated on a Sephadex G-100 column in the presence of PBS, and the fractions containing only Fab and Fc fragments were collected on the basis of their OD value, which was measured spectrophometrically. Finally, Fab fragments were separated from the Fc fragments on a protein A column.

Conjugation of monoclonal antibodies with fluorescent dyes

Aliquots of purified whole mAbs or Fab fragments were conjugated, as described previously, with FITC and tetramethylrhodamine isothiocyanate (TRITC; Molecular Probes, Eugene, OR) (14, 23–25). The dye to protein labeling ratios varied between 2 and 4 for the mAbs and between 0.7 and 1 for the Fab fragments. The labeling ratios were separately determined for each labeled aliquot by spectrophotometric measurements (14). The fluorescently tagged Abs retained their biologic activity according to competition with identical, but unlabeled, Abs in binding to live cell membranes.

[4] Abbreviations used in this paper: FCET, flow cytometric energy transfer; TRITC, tetramethylrhodamine isothiocyanate; ICAM, intercellular adhesion molecule.

Labeling of cells with monoclonal Abs

Cells (1×10^6) in PBS (generally in volumes of 50 μl) were added to predetermined, saturating amounts of mAbs, followed by incubation on ice for 40 min in the dark. To avoid possible aggregation of the Abs and unwanted temperature effects, the Abs were air-fuged (at 10^5 rpm for 30 min) before labeling. The samples were resuspended in 0.5 ml of PBS, supplemented with an equal volume of 2% formaldehyde after washing free from the unbound mAbs. Data obtained with the fixed cells did not differ significantly from those from unfixed, viable cells regardless of whether labeling was conducted before or after fixation.

The number of binding sites on the cell surface was determined from the mean values of flow cytometric histograms of cells labeled to saturation with FITC-conjugated mAbs. The mean fluorescence intensities were converted to numbers of binding sites by calibration with fluorescent microbeads (Quantum 25 from the Flow Cytometry Standards Corp., San Juan, Puerto Rico). The diameter of the JY cells varied between 20 and 25 μm, as assessed by forward light scatter intensity after calibration with microbeads as well as microscopic measurements.

Measurement of the FCET between labeled cell surface proteins

A modified Becton Dickinson FACStar Plus flow cytometer (Becton Dickinson, Mountain View, CA) equipped with dual wavelength excitation from a single argon ion laser (Spectra-Physics Inc., Mountain View, CA) was used to determine fluorescence resonance energy transfer between FITC- and TRITC-conjugated mAbs or Fab fragments bound to the cell surface. A detailed description of the method was previously reported (14, 15–20). Briefly, the labeled cells were excited sequentially at 514 and 488 nm. Fluorescence intensities emitted at 540 ± 10 and >580 nm were detected using a combination of suitable filters. Four intensities were detected and stored for calculation; the fluorescence emissions at 540 ± 10 and >580 nm, both excited at 488 nm; the fluorescence above 580 nm excited at 514 nm; and the small angle forward light scatter intensity of the 514-nm laser line. Correction parameters were obtained from data collected from cells labeled only with FITC- or TRITC-conjugated mAbs. The necessary parameters were collected in list mode and analyzed as previously described (15, 16, 20).

The calculated transfer efficiency was expressed as a percentage of the excitation energy taken up by the donor (in our case the FITC dye) and tunneled to the acceptor (in our case the TRITC dye) molecules (26, 27). The transfer efficiency has an inverse sixth power dependence on the donor-acceptor distance, where the orientation factor of the donor's excitation and the acceptor's emission dipoles can be considered a statistical average of isotropic random orientations, i.e., two-thirds (28, 29). The calculated transfer efficiency has an extremely high sensitivity to changes in distances in the range of 2 to 10 nm (26, 27). Larger energy transfer efficiencies determined between fluorescently labeled mAbs may reflect close physical proximities or larger densities of labeled acceptor molecules in the vicinity of donors if some particular spectroscopic conditions are fulfilled (26–29). The calculated energy transfer, i.e., the proximity of the donor- and acceptor-conjugated Abs was determined on a cell by cell basis and displayed as energy transfer frequency distributions. Additionally, mean values of the energy transfer distribution curves were determined. These data were used and tabulated as characteristic energy transfer efficiencies (which reflect proximities) between two epitopes. This procedure minimizes the unwanted effects of biologic variations in the cell population (14–20, 25, 30–33).

Results

Proximities of tetraspan molecules (CD53, CD81, and CD82) and CD20 to MHC class II molecules

High energy transfer values were measured from FITC-labeled mAbs bound to CD53, CD81, and CD82 and to two different TRITC-labeled mAbs bound to DR on the JY cell surface, but not to TRITC-labeled mAb to CD71 (transferrin receptor; Table I*A* and Fig. 1, *A–F*). Similarly, low FRET efficiency values were measured between CD54 (ICAM-1) and CD81 or CD53 (Table I*A*).

As the membrane topology of the tetraspan proteins is probably similar to that of another important B cell surface molecule, CD20 (34), we similarly examined energy transfer from CD20 to DR and CD71. High energy transfer efficiencies were obtained in both cases (Table I*B* and Fig. 1, *G* and *H*).

Next we examined energy transfer in the reverse direction, i.e., from FITC-labeled mAbs bound to MHC class II molecules (in

Table I. *Energy transfer efficiency values between donor-acceptor pairs*

Donor (FITC-Labeled)		Acceptor (TRITC-Labeled)		
mAb	Antigen	mAb	Antigen	E ± Δ E (%)[a]
Part A				
MEM-53	CD53	MEM-137	DR(α)	20.8 ± 1.8
M38	CD81	MEM-137	DR(α)	14.1 ± 0.6
C33	CD82	MEM-137	DR(α)	12.3 ± 0.4
MEM-53	CD53	L243	DR	7.7 ± 2.4
M38	CD81	L243	DR	8.1 ± 1.3
C33	CD82	L243	DR	7.2 ± 3.5
MEM-53	CD53	anti-CD71	CD71	1.7 ± 2.0
M38	CD81	anti-CD71	CD71	3.3 ± 1.3
C33	CD82	anti-CD71	CD71	2.8 ± 1.8
MEM-112	CD54	M38	CD81	3.8 ± 1.2
MEM-112	CD54	MEM-53	CD53	5.9 ± 1.2
Part B				
MEM-97	CD20	MEM-137	DR(α)	16.2 ± 0.9
MEM-97	CD20	L243	DR	10.1 ± 1.6
MEM-97	CD20	anti-CD71	CD71	15.4 ± 1.9
Part C				
L243	DR	MEM-53	CD53	8.8 ± 0.8
L243	DR	M38	CD81	6.8 ± 0.1
L243	DR	MEM-97	CD20	6.3 ± 0.1
Leu10	DQ	MEM-53	CD53	14.2 ± 1.6
Leu10	DQ	MEM-97	CD20	13.6 ± 1.6
Part D				
BBM.1	β_2-microglobulin	W6/32	MHC-I	11.0 ± 0.9
L368	β_2-microglobulin	W6/32	MHC-I	13.1 ± 0.8
Part E				
L243[b]	DR	L243	DR	6.5 ± 0.9
L243	DR	L368	β_2-microglobulin	11.0 ± 1.5
L368	β_2-microglobulin	L243	DR	11.2 ± 1.3
Part F				
MEM-97	CD20	W6/32	MHC-I	13.7 ± 2.4
MEM-53	CD53	W6/32	MHC-I	13.6 ± 3.1
M38	CD81	W6/32	MHC-I	8.3 ± 4.6
C33	CD82	W6/32	MHC-I	4.4 ± 0.1
MEM-97	CD20	L368	β_2-microglobulin	14.7 ± 2.3
MEM-53	CD53	L368	β_2-microglobulin	13.6 ± 3.5
Part G				
W6/32	MHC-I	MEM-97	CD20	7.9 ± 0.1
W6/32	MHC-I	MEM-53	CD53	7.0 ± 1.5
W6/32	MHC-I	M38	CD81	4.8 ± 1.4
Part H				
W6/32	MHC-I	L243	DR	9.7 ± 1.4
L243	DR	W6/32	MHC-I	9.8 ± 1.2
Leu10	DQ	L243	DR	8.4 ± 0.8
W6/32[b]	MHC-I	W6/32	MHC-I	8.4 ± 0.8
Part I				
MEM-97[b]	CD20	MEM-97	CD20	2.9 ± 2.5
MEM-53[b]	CD53	MEM-53	CD53	2.3 ± 0.6
M38[b]	CD81	M38	CD81	1.5 ± 0.2
Part J				
MEM-97	CD20	MEM-53	CD53	5.6 ± 0.7
MEM-53	CD53	MEM-97	CD20	8.8 ± 2.9
M38	CD81	MEM-53	CD53	3.2 ± 0.8
MEM-53	CD53	M38	CD81	1.1 ± 1.0
MEM-97	CD20	M38	CD81	3.2 ± 0.8
C33	CD82	M38	CD81	2.9 ± 0.4
C33	CD82	MEM-53	CD53	5.4 ± 0.6
Part K				
C33 (Fab)	CD82	L243 (Fab)	DR	8.5 ± 1.3
MEM-53 (Fab)	CD53	L243 (Fab)	DR	12.4 ± 1.3
MEM-53 (Fab)	CD53	W6/32 (Fab)	MHC-I	13.1 ± 2.4
M38 (Fab)	CD81	W6/32 (Fab)	MHC-I	7.2 ± 0.4
C33 (Fab)	CD82	W6/32 (Fab)	MHC-I	16.9 ± 2.9
BBM.1 (Fab)	β_2-microglobulin	W6/32 (Fab)	MHC-I	11.1 ± 0.8
W6/32 (Fab)	MHC-I	W6/32 (Fab)	MHC-I	8.0 ± 0.5
MEM-137 (Fab)	DR(α)	W6/32 (Fab)	MHC-I	13.4 ± 1.0

[a] Data represent mean ± SEM of at least four independent experiments.
[b] In the case of competing mAbs, care was taken that half of the available binding sites be occupied by the TRITC-labeled Ab.

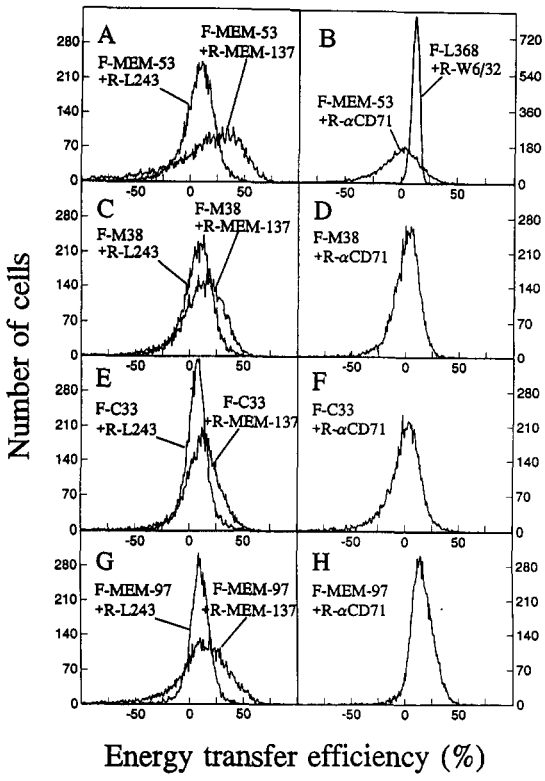

FIGURE 1. Frequency distribution curves of FCET efficiencies measured between FITC-conjugated mAbs bound to tetraspan molecules and TRITC-conjugated mAbs bound to DR, DR(α), and CD71. The energy transfer between FITC-L368 (anti-β_2m) and TRITC-W6/32 (anti-MHC class I heavy chain) serves as the positive control, and that between FITC-mAbs specific to tetraspan molecules and TRITC-anti-CD71 serves as the negative control. F, FITC-conjugated; R, TRITC-conjugated.

this case DR and DQ) toward TRITC-labeled mAbs bound to some tetraspan molecules or to CD20. High values of energy transfer in this arrangement confirmed the mutual proximity of these molecules (Table I*C*).

The energy transfer efficiencies were comparable to the positive control, i.e., energy transfer between mAbs to two different epitopes in MHC class I molecules (Table I*D* and Fig. 1*B*).

A straightforward interpretation of these results is that CD53, CD81, CD82, and CD20 are all in close proximity to DR (more

Table II. *Negative and positive cooperativity between FITC-labeled antibodies bound to CD20 and tetraspan molecules (CD53, CD81, CD82) on JY cells*

mAb_1 (Antigen)	$mAb(s)_2$ (Antigen)	$100 \times (I - I_0)/I_0$[a]
Part A		
MEM-97 (CD20)	MEM-53 (CD53)	−13.9 ± 7.0
MEM-97 (CD20)	C33 (CD82)	−16.7 ± 1.5
MEM-97 (CD20)	MEM-53 (CD53) + M38 (CD81) + C33 (CD82)[b]	−11.9 ± 1.0
MEM-53 (CD53)	M38 (CD81)	9.9 ± 4.3
MEM-53 (CD53)	M38 (CD81) + C33 (CD82)[b]	7.1 ± 2.1
MEM-53 (CD53)	C33 (CD82)	4.2 ± 3.1
M38 (CD81)	C33 (CD82)	−17.9 ± 3.5
Part B		
MEM-53 (CD53)	anti-CD71 (CD71)	2.2 ± 1.7
MEM-53 (CD53)	MEM-112 (CD54)	0.1 ± 2.5
M38 (CD81)	MEM-112 (CD54)	3.9 ± 0.2

[a] Designations: I_0, the sum of mean fluorescence intensities of flow cytometric histograms collected from cells labeled with either FITC-mAb_1 or FITC-$mAb(s)_2$ alone; I, the mean fluorescence intensity of flow cytometric histogram collected from cells simultaneously labeled with FITC-mAb_1 and FITC-$mAb(s)_2$. Data represent mean ± SEM of at least three experiments.

[b] This designation means simultaneous labeling with the listed mAbs.

specifically the DRα-chain), and at least CD53 and CD20 are also close to DQ. (CD81 and CD82 were not examined in this series of experiments for technical reasons.) Significantly higher energy transfer to DR from CD53 and CD20 than that from CD81 and CD82 indicates that CD53 and CD20 are closer to DR than is CD81 or CD82. These differences could also be due to different orientations of the epitopes in the individual tetraspan molecules and CD20 toward DR.

A slight competition (negative cooperativity of binding probably due to steric hindrance) between some tetraspans and CD20 and between CD81 and CD82 was observed (Table II*A*), reinforcing the idea of the mutual vicinity of these molecules.

Different efficiencies of energy transfer from FITC-conjugated mAbs to tetraspans and CD20 toward two different TRITC-conjugated mAbs to DR indicate a type of sidedness in the interactions among tetraspans, CD20, and DR; the MEM-137 epitope on the α-chain appears to be closer to the tetraspan complex than the L243 epitope (Table I*A* and Fig. 1, *A*, *C*, *E*, and *G*).

Significant energy transfer values between the same mAbs against DR indicate that a part of these molecules is homoassociated (Table I*E*). However, it is not a priori clear whether these

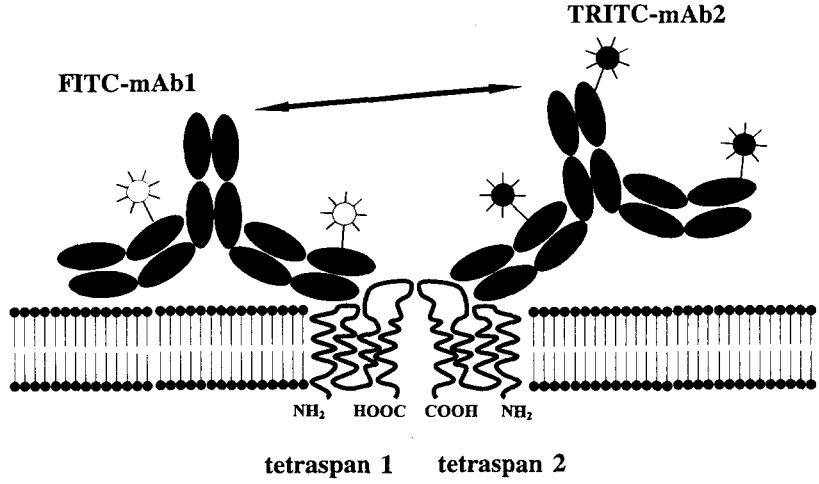

FIGURE 2. Schematic drawing of a tetraspan-tetraspan dimer displaying possible steric relationships among the Ags and among the mAbs bound to them. Note that tetraspan molecules are oversized compared with IgGs to demonstrate the four membrane-spanning segments.

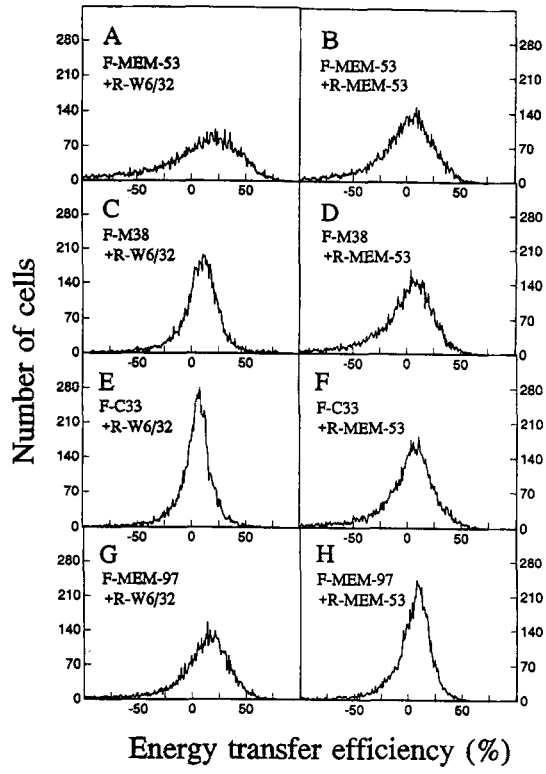

FIGURE 3. Frequency distribution curves of FCET efficiencies measured between FITC-conjugated mAbs bound to tetraspan molecules and TRITC-conjugated mAb bound to MHC class I Ag as well as between FITC- and TRITC-conjugated mAbs bound to members of the tetraspan family. F, FITC-conjugated; R, TRITC-conjugated.

homoassociated DR molecules are specifically those involved in the interactions with tetraspans and CD20. We could also demonstrate the heteroassociation of HLA class I and II molecules, reconfirming our previous observation (14) (Table I, *E* and *H*).

Proximities of tetraspan molecules and CD20 to MHC class I antigens

Previously, it was shown that fractions of MHC class I and class II molecules are associated on the B cell surface (14). Therefore, we investigated whether MHC class I proteins may also be similarly associated with tetraspan molecules and CD20. Indeed, high energy transfer values were observed from FITC-labeled mAbs against CD20, CD53, and CD81 toward two different TRITC-labeled mAbs against MHC class I (Table I*F* and Fig. 3, *A*, *C*, *E*, and *G*). However, the efficiency of energy transfer was significantly lower when the donor vs acceptor molecules were reversed (i.e., transfer from FITC-labeled mAbs to MHC class I toward TRITC-labeled mAbs to CD20 or tetraspans; Table I*G*). This can obviously be attributed to a great change in the acceptor/donor ratio (Table III).

The fact that high energy transfer was observed between MHC class I and class II on the same cells (Table I*H*) makes it likely that multicomponent complexes composed at least of MHC class I, MHC class II, CD20, CD53, CD81, and CD82 exist on the JY cell surface.

Energy transfer between tetraspan molecules and CD20

No significant energy transfer was observed between the same mAbs bound to CD53, CD81, or CD20, indicating the lack of homoassociations of these molecules (Table I*I* and Fig. 3*B*). Energy transfer among various molecules of this set was larger, but in most cases (except energy transfer from FITC-MEM-97 (against CD20) toward TRITC-MEM-53 (against CD53)) it was rather low, on the borderline of significance (Table I*J* and Fig. 3*H*). The results either indicate that the tetraspan molecules and CD20 are not sufficiently close to each other in the complexes with MHC molecules or that the epitopes are unfavorably positioned so that the mAbs bound to them point away from each other. Another possibility is that there are significant constraints on the orientation of the mAbs bound very close to the surface of the membrane, which is to be expected in the case of molecules such as tetraspans and CD20, in which only a minor part protrudes from the membrane (Fig. 2). These data can also be considered as negative controls, indicating that energy transfer occurs only if the properly oriented donor-acceptor pairs are at molecular vicinity. Due to the multiple labeling of mAbs, a random orientation of donors and acceptors can be assumed.

Table III. *Number of binding sites of some antibodies on the JY cell surface*

mAb	Antigen	Number of Binding Sites ($\times 10^3$)
W6/32	MHC-I	1034 ± 70[a]
L368	β_2-microglobulin	684 ± 74
L243	DR	420 ± 40
MEM-137	DR(α)	335 ± 82
Leu10	DQ	63 ± 4
MEM-97	CD20	68 ± 11
MEM-53	CD53	78 ± 8
M38	CD81	69 ± 6
MEM-112	CD54 (ICAM-1)	53 ± 9
C33	CD82	51 ± 6
anti-CD71	CD71	44 ± 4

[a] Data represent mean ± SEM of at least four independent measurements.

Positive and negative cooperativity between mAbs binding to tetraspan molecules and CD20

The sum of fluorescence intensities from FITC-labeled mAbs to two different, completely independent surface molecules should be the same regardless of whether both mAbs bound to a single cell simultaneously or one after the other, i.e., sequentially. If there is a difference, there must be some kind of physical relationship between the two molecules, if we exclude the possibilities of indirect effects, e.g., by mild fixation of the cell membrane. As shown in Table II*A*, significant negative or positive cooperativity was observed when pairs of relevant mAbs were tested in this way. However, these phenomena were not observed between mAbs against some tetraspans on the one side and mAbs against CD71 or CD54 (ICAM-1) on the other (Table II*B*). These results indicate that some mAbs against tetraspan molecules and CD20 are not independent, but communicate with each other, probably due to their proximity. The negative cooperativity can be due to partial competition (sterical hindrance) or to fluorescence quenching due to close proximity. On the other hand, the positive cooperativity (between MEM-53 (against CD53) and M38 (against CD81)) may be due to the slightly altered affinity of binding caused by perturbation (conformational change) of the adjacent Ags by their interactions with mAbs. In any case, these data argue for mutual proximity of CD20, CD53, CD81, and CD82. To show the abundance of various epitopes on the JY cell surface, the numbers of binding sites of some Abs are summarized in Table III.

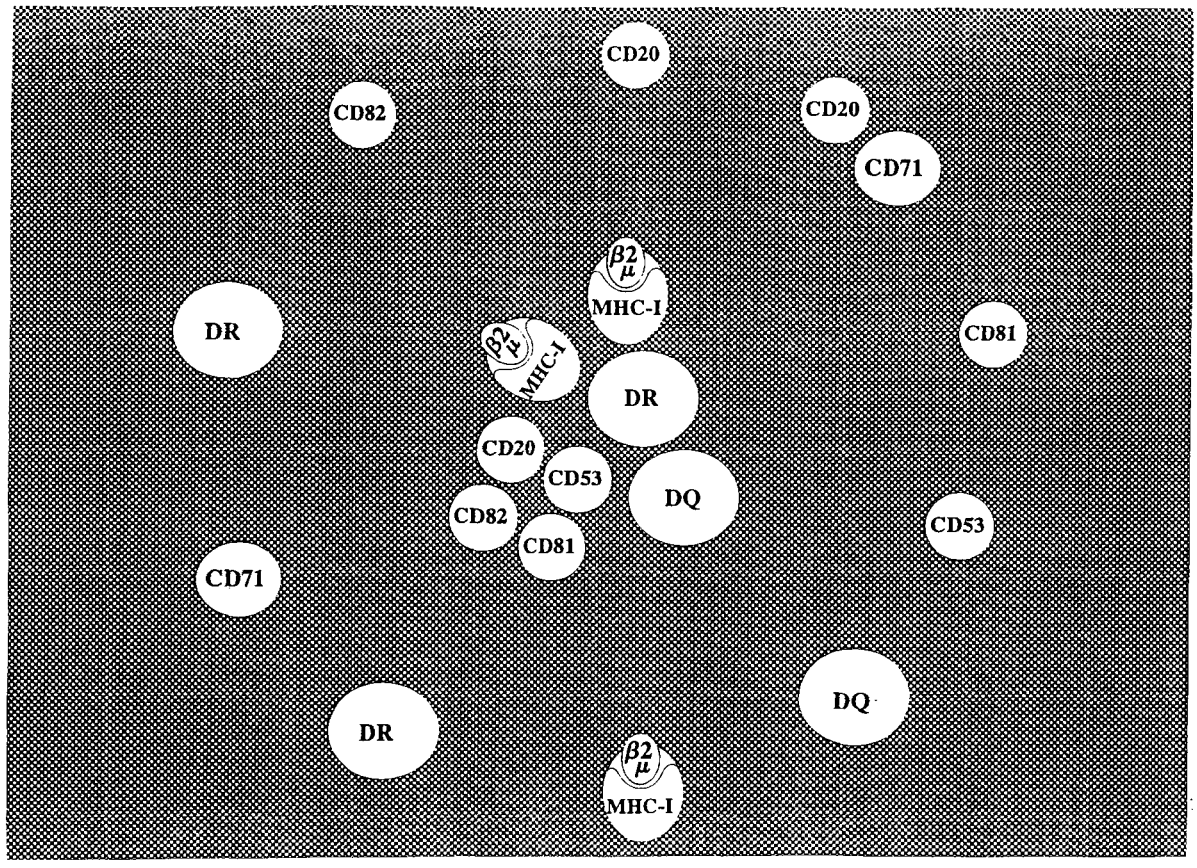

FIGURE 4. A hypothetical schematic model of proximity relationships among the JY surface molecules examined in this study. Many other B cell surface molecules that were not examined are not shown here. For further explanation, see *Discussion*.

The proximities observed are not induced by antibody cross-linking

Essentially identical results were obtained when Fab fragments of mAbs against CD53, CD81, CD82, and MHC class II and class I were used (Table I*K*) instead of whole fluorescently labeled mAbs, indicating that the proximities of the membrane molecules observed were not due to Ab-induced cross-linking. In addition, the proximity data were independent of the mild fixation of the cells by 1% formaldehyde, either before or after labeling (data not shown). Finally, these results are in good agreement with the previous biochemical results on co-isolation of tetraspan molecules with MHC class II (13); we recently observed co-isolation of small amounts of CD20 and MHC class I with the tetraspan-MHC class II complexes after JY cell solubilization in a mild detergent 3-[(3-cholamidopropyl)dimethylammonio]-1-propanesulfonate (P. Angelisová, unpublished observation).

Discussion

The results presented here confirm by in situ biophysical methods, with the capacity to provide data on a cell by cell basis, the previous biochemical data on the association of three tetraspan molecules (CD53, CD81, and CD82) with MHC class II Ags (13) on the surface of a B cell line.

In addition, we found that two other important B cell surface molecules, CD20 and MHC class I, take part in these supramolecular structures. CD20 is a protein whose polypeptide chain presumably also crosses the membrane four times (34). MHC class I molecules have been previously found to be associated with MHC class II glycoproteins (14).

Evaluation of the energy transfer efficiencies among various pairs of the molecules examined here made it possible to construct a hypothetical model of a multicomponent complex on the B cell surface, as shown in Figure 4. This model is a minimalistic one, as other proteins are likely to be present in the complex. One of them is another tetraspan protein, CD37, which was co-isolated with MHC class II proteins and the other tetraspan proteins after mild detergent solubilization (13), but for technical reasons (lack of suitable labeled mAbs in sufficient amounts) has not been studied in the present work. The same may be true for CD19 and CD21 (10, 13).

It should be noted that significant energy transfer efficiencies indicate proximities of the donor and acceptor (i.e., rough proximities between the two epitopes) below 10 nm. A well-defined control included in our measurements was the MHC class I molecule, namely the epitopes recognized by the W6/32 mAb (directed at an epitope in the α-chain) and mAbs L368 and BBM.1 (recognizing epitopes in the β_2m). The energy transfer efficiency in this case was approximately 11 to 13% (Table I*D*). Theoretical calculations employing the basic equations describing FCET (16, 18, 19) yield the distance of 7.6 nm between the donor and the acceptor for the energy transfer efficiency of 13% under idealized conditions (donor to acceptor ratio of 1:1, no restrictions in the flexibility of the labeled Abs bound to the membrane molecules, equal level of fluorescent labels on both mAbs, etc.). This value is in good agreement with the MHC class I molecule dimensions ($\sim 4 \times 5 \times 7$ nm) (35), taking into consideration the size of the IgG molecules as well. The energy transfer efficiencies of 4 to 20% observed in the present study would roughly correspond (under

similar idealized conditions) to epitope distances between 9 and 7 nm, respectively. It is somewhat surprising that in some cases higher energy transfer efficiencies were observed between fluorescently labeled mAbs bound to different molecules than between those bound to different epitopes of the same molecules (MHC class I). This fact simply indicates that the intermolecular distances within these complexes are comparable to those of intermolecular epitopes, i.e., very close. The efficiency of the energy transfer is known to be dependent mainly on the acceptor concentration (16, 18, 20). The total surface density of the MHC molecules is much higher than that of the tetraspan molecules (Table III), yet the energy transfer efficiencies in both directions (from tetraspans to MHC molecules and vice versa) are of comparable magnitude (Table I, *B*, *K*, and *C*). This indicates that only a fraction of the MHC molecules is in the vicinity of tetraspans, while a relatively large part of the tetraspan proteins may be close to the MHC molecules.

The present study confirmed our previous results on co-association of the tetraspan proteins with MHC class II molecules (13), but somewhat surprisingly revealed that at least two other molecules are present in these complexes, namely CD20 and MHC class I. Recently, we have examined whether these proteins can be detected in the materials isolated on anti-CD53 and anti-CD81 immunosorbents from B cell line lysates. Indeed, small amounts of both CD20 and MHC class I could be detected in these preparations by Western blotting (P. Angelisová, unpublished observations).

In most cases, relatively low energy transfer efficiencies were detected between the different tetraspan molecules (including CD20). Because of the significant cooperativity effects of binding of mAbs to the investigated tetraspan molecules (Table II*A*), we suggest that these molecules are in close vicinity to each other, but the orientation of the epitopes recognized by the fluorescently labeled mAbs is probably unfavorable (i.e., the mAbs may point markedly out of each other; see Fig. 2). Also, mAbs to the tetraspan molecules may (due to small size of the extracellular domains of the tetraspans) significantly interact with lipid moieties of the cell membrane, which may limit their flexibility and keep them in rather fixed positions.

Potential effects of aggregation of the studied molecules by the bivalent mAbs or effects of indirect aggregation due to simultaneous interactions of the mAbs with Fc receptors seem unlikely, as similar results were obtained with Fab fragments; furthermore, essentially identical results were obtained whether unfixed or (before or after labeling) formaldehyde-fixed cells were used for the measurements with whole Abs.

Our model shown in Figure 4 suggests that only a fraction of the relevant molecules is involved in these complexes, while another fraction is uncomplexed or associated with other molecules; for example, our present data indicate the existence of complexes involving CD20 and CD71 (transferrin receptor; Table I*B*), which is also represented in Figure 4. Other B cell surface molecules have been previously shown to be in mutual proximity, such as MHC class II and CD54 (ICAM-1; not shown in Fig. 4) (36).

Because of the reasons discussed above (certain differences in the fluorescent labeling of various mAbs, large differences in the surface density of the donor and acceptor molecules, and possible sterical restrictions on flexibility of the Ab molecules bound to some of the membrane molecules), this model is very tentative; a safe interpretation of our results is simply that the molecules are close to each other. Elucidation of finer structural details of these multicomponent complexes will require refinement of the tools used as well as additional techniques.

Although the FCET method can provide valuable data on in situ proximities of cell surface molecules, it does not yield enough information on some aspects, such as: What fractions of the total DR, DQ, MHC class I, CD20, CD53, CD81, and CD82 molecules are involved in these complexes? What is the stoichiometry of these complexes? Is there any possible heterogeneity in these complexes (i.e., do all of these complexes have the same composition or are there also incomplete complexes lacking some of the components, in accordance with the different densities of the molecules at the cell membrane?)? For example, it is difficult to assess whether all energy transfer from DR to DQ or from MHC class I to MHC class I is only due to the molecules present in the MHC tetraspan complexes or whether a fraction of independent, simpler complexes such as DR-DQ or MHC I-MHC I exists that is devoid of tetraspan components. The previous biochemical experiments with detergent-solubilized cell membranes suggest that only minor fractions of the total DR and CD82, but substantial fractions of the total CD81 (and CD37), are present in these complexes (13). The total lack of energy transfer from CD53 to CD53, CD81 to CD81, and CD20 to CD20 (Table I*I* and Fig. 3*B*) indicates that the complexes either contain only single molecules of CD20, CD53, and CD81 or, if there are multiple CD20, etc., they are more than 10 nm from each other. The higher the deviation between the individual densities of the studied proteins, the larger the likelihood that the measured patterns are not the only possibilities for expression of the individual molecules in the cell membrane. Recently, a higher level of supramolecular organization of the human MHC class I molecules was demonstrated at the surface of JY cells. That means that the individual receptor islands may be further organized into island groups (37).

In any case, the present and previous data suggest that the B cell surface membranes contain large multicomponent complexes involving MHC class I and class II proteins, CD20, several tetraspan molecules, and possibly other components. It is tempting to speculate that these supramolecular assemblies might be involved in Ag presentation to T cells and in signaling to the B cell via the MHC molecules contacted by the TCR. CD20 was demonstrated to be a component of B cell surface Ca^{2+} channels (38), and the structures of the tetraspan proteins are also compatible with such a function. It remains to be explored whether the tetraspan complexes might, for example, serve as MHC protein-linked ion channels.

Acknowledgments

We thank all donors of the cells and Abs in this study.

References

1. Wright, M. D., and M. G. Tomlinson. 1994. The ins and outs of the transmembrane 4 superfamily. *Immunol. Today 15:588.*
2. Dong, J.-T., P. W. Lamb, C. W. Rinker-Schaeffer, J. Vukanovic, T. Ichikawa, J. T. Isaac, and J. C. Barrett. 1995. KAI1, a metastasis suppressor gene for prostate cancer on human chromosome 11p11.2. *Science 268:884.*
3. Ikeyama, S., M. Koyama, M. Yamaoko, R. Sasada, and M. Miyake. 1993. Suppression of cell motility and metastasis by transfection with human motility-related protein (MRP-1/CD9) DNA. *J. Exp. Med. 177:1231.*
4. Rubinstein, E., F. LeNaour, M. Billard, M. Prenant, and C. Boucheix. 1994. CD9 antigen is an accessory subunit of the VLA integrin complexes. *Eur. J. Immunol. 24:3005.*
5. Kitani, S., E. Berenstein, S. Mergenhagen, P. Tempst, and R. P. Siraganian. 1991. A cell surface glycoprotein of rat basophilic leukemia cells close to the high affinity IgE receptor (FcεRI): similarity to human melanoma differentiation antigen ME491. *J. Biol. Chem. 266:1903.*
6. Bell, G. M., W. E. Seaman, E. C. Niemi, and J. B. Imboden. 1992. The OX-44 molecule couples to signaling pathways and is associated with CD2 on rat T lymphocytes and a natural killer cell line. *J. Exp. Med. 175:527.*
7. Imai, T., M. Kakizaki, M. Nishimura, and O. Yoshie. 1995. Molecular analyses of the association of CD4 with two members of the transmembrane 4 superfamily, CD81 and CD82. *J. Immunol. 155:1229.*
8. Takahashi, S., C. Doss, S. Levy, and R. Levy. 1990. TAPA-1, the target of an antiproliferative antibody, is associated on the cell surface with the Leu-13 molecules. *J. Immunol. 149:2841.*
9. Bradbury, L. E., G. S. Kansas, S. Levy, R. L. Evans, and T. F. Tedder. 1992. The CD19/CD21 signal transducing complex of human B lymphocytes includes the

target of antiproliferative antibody-1 and Leu-13 molecules. *J. Immunol. 149: 2841.*
10. Bradbury, L. E., V. S. Goldmacher, and T. F. Tedder. 1993. The CD19 signal transduction complex of B lymphocytes. *J. Immunol. 151:2915.*
11. Matsumoto, A. K., D. R. Martin, R. H. Carter, L. B. Klickstein, J. M. Ahearn, and D. T. Fearon. 1993. Functional dissection of the CD21/CD19/TAPA-1/Leu-13 complex of B lymphocytes. *J. Exp. Med. 178:1407.*
12. Shick, M. R., and S. Levy. 1993. The TAPA-1 molecule is associated on the surface of B cells with HLA-DR molecules. *J. Immunol. 151:4090.*
13. Angelisová, P., I. Hilgert, and V. Hořejší. 1994. Association of four antigens of the tetraspans family (CD37, CD53, TAPA-1, and R2/C33) with MHC class II glycoproteins. *Immunogenetics 39:249.*
14. Szöllősi, J., S. Damjanovich, M. Balázs, P. Nagy, L. Trón, M. J. Fulwyler, and F. M. Brodsky. 1989. Physical association between MHC class I and class II molecules detected on the cell surface by flow cytometric energy transfer. *J. Immunol. 143:208.*
15. Szöllősi, J., L. Trón, S. Damjanovich, S. H. Helliwell, D. J. Arndt-Jovin, and T. M. Jovin. 1984. Fluorescence energy transfer measurements on cell surfaces: a critical comparison of steady-state fluorimetric and flow cytometric methods. *Cytometry 5:210.*
16. Trón, L., J. Szöllősi, S. Damjanovich, S. H. Helliwell, D. J. Arndt-Jovin, and T. M. Jovin. 1984. Flow cytometric measurement of fluorescence resonance energy transfer on cell surfaces: quantitative evaluation of the transfer efficiency on a cell-by-cell basis. *Biophys. J. 45:939.*
17. Szöllősi, J., L. Mátyus, L. Trón, M. Balázs, I. Ember, M. J. Fulwyler, and S. Damjanovich. 1987. Flow cytometric measurements of fluorescence energy transfer using single laser excitation. *Cytometry 8:120.*
18. Szöllősi, J., S. Damjanovich, S. A. Mulhern, and L. Trón. 1987. Fluorescence energy transfer and membrane potential measurements monitor dynamic properties of cell membranes: a critical review. *Prog. Biophys. Mol. Biol. 49:65.*
19. Trón, L., J. Szöllősi, and S. Damjanovich. 1987. Proximity measurements of cell surface proteins by fluorescence energy transfer. *Immunol. Lett. 16:1 (Rev.).*
20. Matkó, J., J. Szöllősi, L. Trón, and S. Damjanovich. 1988. Luminescence spectroscopic approaches in studying cell surface dynamics. *Q. Rev. Biophys. 21:479.*
21. Terhorst, C., P. Parham, D. L. Mann, and J. L. Strominger. 1979. Structure of HLA antigens: amino-acid and carbohydrate compositions and NH_2-terminal sequences of four antigen preparations. *Proc. Natl. Acad. Sci. USA 73:910.*
22. Edidin, M., and T. Wei. 1982. Lateral diffusion of H-2 antigens on mouse fibroblasts. *J. Cell Biol. 95:458.*
23. De Petris, S. 1978. Immunoelectron microscopy and immunofluorescence in membrane biology. In *Methods in Membrane Biology*, Vol. 9. E. D. Korn, ed. Plenum Press, New York, pp. 1–201.
24. Spack, E. G., Jr., B. Packard, M. L. Wier, M. Edidin. 1986. Hydrophobic adsorption chromatography to reduce nonspecific staining by rhodamine-labeled antibodies. *Anal. Biochem. 158:233.*
25. Szöllősi, J., S. Damjanovich, C. K. Goldman, M. J. Fulwyler, A. A. Aszalós, G. Goldstein, P. Rao, M. Talle, and T. A. Waldmann. 1987. Flow cytometric resonance energy transfer measurements support the association of a 95-kDa peptide termed T27 with the 55-kDa Tac peptide. *Proc. Natl. Acad. Sci. USA 84:7246.*
26. Stryer, L. 1978. Fluorescence energy transfer as a spectroscopic ruler. *Annu. Rev. Biochem. 47:819.*
27. Cantor, C., and R. Schimmel. 1980. *Biophysical Chemistry*, Vol. II: *Fluorescence Spectroscopy*. Freeman, Inc., San Francisco, p. 433.
28. Dale, R. E., and J. Eisinger. 1976. Intramolecular energy transfer and molecular conformation. *Proc. Natl. Acad. Sci. USA 73:271.*
29. Dale, R. E., J. Eisinger, and W. E. Blumberg. 1979. The orientational freedom of molecular probes. The orientation factor in intramolecular energy transfer. *Biophys. J. 26:161.*
30. Liegler, T., J. Szöllősi, W. Hyun, and R. S. Goodenow. 1991. Proximity measurements between H-2 antigens and the insulin receptor by fluorescence energy transfer: evidence that a close association does not influence insulin binding. *Proc. Natl. Acad. Sci. USA 88:6755.*
31. Mátyus, L. 1992. Fluorescence resonance energy transfer measurements on cell surfaces: a spectroscopic tool for determining protein interactions. *Photochem. Photobiol. 12:323.*
32. Damjanovich, S., J. Szöllősi, and L. Trón. 1992. Transmembrane signaling in T cells. *Immunol. Today 13:A12.*
33. Damjanovich, S., L. Mátyus, M. Balázs, R. Gáspár, Z. Krasznai, C. Pieri, J. Szöllősi, and L. Trón. 1992. Dynamic physical interactions of plasma membrane molecules generate cell surface patterns and regulate cell activation processes. *Immunobiology 185:337.*
34. Einfeld, D. A., J. P. Brown, M. A. Valentine, E. A. Clark, and J. A Ledbetter. 1988. Molecular cloning of the human B cell CD20 receptor predicts a hydrophobic protein with multiple transmembrane domains. *EMBO J. 7:711.*
35. Bjorkman, P. J., M. A. Saper, B. Samraoui, W. S. Bennett, J. L. Strominger, and D. C. Wiley. 1987. Structure of the human class I histocompatibility antigen, HLA-A2. *Nature 329:506.*
36. Bene, L., M. Balázs, J. Matkó, J. Möst, M. P. Dierich, J. Szöllősi, and S. Damjanovich. 1994. Lateral organization of the ICAM-1 molecule at the surface of human lymphoblasts: a possible model for its co-distribution with the IL-2 receptor, class I and class II HLA molecules. *Eur. J. Immunol. 24:2115.*
37. Damjanovich, S., G. Vereb, A. Schaper, A. Jenei, J. Matko, J. P. P. Starink, G. O. Fox, D. J. Arndt-Jovin, and T. M. Jovin. 1995. Structural hierarchy in the clustering of HLA class I molecules in the plasma membrane of human lymphoblastoid cells. *Proc. Natl. Acad. Sci. USA 92:1122.*
38. Bubien, J. K., K.-J. Zhou, P. D. Bell, R. A. Friz, and T. F. Tedder. 1993. Transfection of the CD20 cell surface molecule into ectopic cell types generates a Ca^{2+} conductance found constitutively in B lymphocytes. *J. Cell Biol. 121:1121.*